Journal of Nuclear Materials 517 (2019) 71–79

Contents lists available at ScienceDirect

Journal of Nuclear Materials

journal homepage: www.elsevier.com/locate/jnucmat

# Silver iodide sodalite – Wasteform / Hip canister interactions and aqueous durability

E.R. Maddrell [a, *], E.R. Vance [b], C. Grant [b], Z. Aly [b], A. Stopic [b], T. Palmer [b], J. Harrison [b], D.J. Gregg [b]

[a] National Nuclear Laboratory, Sellafield, Seascale, Cumbria, CA20 1PG, UK
[b] ANSTO, Locked Bag 2001, Kirrawee DC, NSW, 2232, Australia

## HIGHLIGHTS

- Iodine loaded silver exchanged zeolite converts to silver sodalite-rich wasteform after HIPping in Cu or Ni canisters.
- Interfacial reaction zones ~100–200 μm form between the wasteform and both Cu and Ni HIP canisters.
- Durability testing indicates that the wasteform is highly resistant to leaching in deionised water.
- Silver sodalite is destabilised under reducing groundwater conditions that may occur in geological disposal facilities.

## ARTICLE INFO

*Article history:*
Received 2 November 2018
Received in revised form
30 January 2019
Accepted 2 February 2019
Available online 4 February 2019

## ABSTRACT

The use of silver zeolite for the capture of radioiodine from the vapour phase, followed by thermal conversion now appears to be the most direct route by which a sodalite wasteform can be formed. In addition, consolidation by hot-isostatic pressing (HIP) in sealed canisters has many significant advantages over conventional methods such as sintering or melting these candidate wasteforms. The choice of HIP canister material is important as reaction at the wasteform/HIP canister interface results in an interaction zone that can potentially produce detrimental phases, wasteform porosity and canister thinning. This paper builds on a previous study that demonstrated that iodine could be captured from the vapour phase using silver exchanged zeolite and converted to sodalite by HIPing in Fe HIP canisters. The Cu or Ni metal HIP canisters used in this work result in an ~100–200 μm thick local interaction zone with a variety of chemistries. Durability studies were conducted using a variety of reducing conditions and clearly demonstrated the redox sensitivity of silver sodalite. While the silver sodalite wasteform produced is, like the popular AgI-based wasteforms, highly leach resistant to leaching by deionised water it was unstable under highly reducing conditions, which are likely to occur in most geological disposal facilities. Post leaching characterisation revealed the redeposition of AgI and the formation of an aluminosilicate alteration layer under some leaching conditions. Appropriate precautions are required should a silver sodalite wasteform for iodine immobilisation be exposed to reducing groundwater conditions.



## 1. Introduction

Current best practice for the management of fission product iodine (both the stable I-127 and the long-lived radioactive I-129 with a 15.7 million year half-life) at a nuclear fuel reprocessing facility is by discharge to sea. This approach is known as dilute and disperse – dilution into a much larger reservoir of natural iodine and dispersal by marine currents. With the anticipated global renaissance of nuclear power and a realisation that once through fuel cycles may be unattractive, it will become necessary to review this strategy. Social and political attitudes will have evolved and future spent fuel processing plants may not always have access to such discharge routes. This may lead to a requirement for the immobilisation of fission product iodine in a durable wasteform and in this regard a review of I-129 immobilisation has recently been published [1,2].

* Corresponding author.
*E-mail address:* ewan.r.maddrell@nnl.co.uk (E.R. Maddrell).

https://doi.org/10.1016/j.jnucmat.2019.02.002
0022-3115/

Several methods have been employed to eliminate radioiodine from the gaseous waste streams from the current PUREX process, including counter-current scrubbing of the off-gas system [3,4]. Solid sorbents have also been extensively studied, such as silver-containing sorbents [5] and most recently silver-exchanged mordenite-type-zeolites [6]. The latter approach has led to the development of silver iodide sodalite, $Ag_4Al_3Si_3O_{12}I$, as a promising wasteform candidate [1,7–11]. Other recently developed wasteform candidates include silver-functionalized silica aerogel, silver-loaded aluminosilicate aerogels, phosphate glasses and CuI [1,12–15].

In previous internally published work [16], XRD indicated a sodalite structured phase was produced by HIPing a mixture of nepheline and silver iodide – albeit with only partial conversion. The reaction targeted to form the sodalite phase was:

$$3\ NaAlSiO_4 + AgI \rightarrow (Na_3Ag)(AlSiO_4)_3I$$

Two recent studies [17,18] have demonstrated that iodine vapour could be captured onto a commercial silver exchanged zeolite (Ionex®-Type Ag 400, $Ag_{84}Na_2Al_{86}Si_{106}O_{384}$) which subsequently converted to a silver sodalite by HIP. Therein we had tried to achieve a uniform distribution of iodine at 85% of the stated capture substrate capacity of 150 mg per g of substrate. A mass balance exercise indicated that at this loading all of the silica and alumina in the zeolite would form sodalite. However, achieving a uniform iodine loading proved impractical and we observed an inhomogeneous iodine distribution. The more iodine rich regions converted to major silver sodalite with AgI inclusions, in agreement with the mass balance exercise; and the iodine-poor (or even free) regions contained silver nepheline. This study attempted to replicate synthesis of the mixed cation sodalite, but attempts were unsuccessful. Nevertheless, the use of silver zeolite followed by thermal conversion now appears to be the most direct route by which a sodalite wasteform can be formed via capture of iodine from the vapour phase.

Recent DFT-based computational studies have suggested that although dilute solid solutions are stable near both end members of the mixed cation iodosodalite series, higher concentrations would undergo phase separation into the two end members [19]. This work highlighted differences in the $M_4I$ clusters that occupy the β cages in the sodalite framework. Based simply on lattice parameter considerations (Ag and Na iodosodalite differ by less than 1%), solid solution would be expected, and it appears that the reason it does not occur is the instability of mixed $(Na,Ag)_4I$ clusters. To put a physical perspective on this, we suggest that an $Na_4I$ cluster has significant ionic character, whilst an $Ag_4I$ cluster is more covalent. Iodine is able to be either ionic or covalent, but cannot be both simultaneously.

The HIP consolidation process also has many significant advantages over the conventional methods (such as sintering or melting) for processing of the iodine-bearing zeolite material. Notably, it reduces the chance of radioiodine release during hot consolidation via use of a sealed HIP canister, thus reducing the off-gas system requirements; there are less secondary wastes; and it produces a fully dense product. At HIPing conditions (high temperatures and high pressure), the wasteform and HIP canister used for containment of the waste material can potentially interact. The standard HIP canister material is austenitic stainless steel and with respect to the Synroc titanates, typically a small interaction zone forms between the HIP canister and the wasteform, but this generally does not destabilise the waste immobilising phases [20,21]. This reaction is driven by chromium, thermodynamically the most reducing component of stainless steel. Previously we have reported such interactions whilst HIPing silver exchanged zeolite using HIP canisters made from Fe [18]. A significant reaction zone 80–100 μm thick was noted between the HIP canister and the wasteform, including oxidation of the Fe canister to iron oxide and reduction of the wasteform producing silver metal with subsequent release of iodine. It is therefore of interest and importance to understand such interactions and their effect on the quality of the wasteform.

In the present study, the feasibility of HIPed silver sodalite as a wasteform and processing route for the immobilisation of radioiodine is further assessed. HIP canisters made from two alternative metals to iron are investigated in an attempt to minimise or eliminate the wasteform/HIP canister interaction. In addition, the durability of a representative sample of the silver iodosodalite based wasteform is assessed under various reducing conditions to further elucidate its known redox sensitivity. In this respect we report results from PCT and MCC-1 type leaching experiments as well as the wasteform surface interaction zone and leached layer composition.

## 2. Experimental details

### 2.1. Materials and iodine loading

As previously described [18], commercial silver exchanged zeolite beads, 1–2 mm diameter, were used which had a stated composition of $Ag_{84}Na_2Al_{86}Si_{106}O_{384}$ (Sigma Aldrich product 382280). Iodine was in the form of resublimed crystals (Alfa Aesar product 41955). The iodine crystals were ground lightly using a pestle and mortar to facilitate a more homogeneous distribution within the capture substrate.

Sample definition was derived from our previous study using commercial silver exchanged zeolite as the capture substrate [18]. Given the impracticality of achieving a uniform iodine distribution below the concentration that leads to complete silver sodalite formation upon HIPing it was decided to saturate the zeolite with iodine. This was achieved by mixing the zeolite with 175 mg iodine per g zeolite compared with the stated capacity of 150 mg.

The required amount of iodine was added to a robust Teflon bottle, the zeolite added rapidly to the bottle to minimise water absorption on exposure to the atmosphere, and the bottle lid secured. The Teflon bottle was warmed in an oven to 140 °C overnight to achieve the required reaction between silver and iodine. The following morning the bottle was cooled and the lid removed, then returned to the oven to allow any excess iodine to be volatilised. Measuring the mass gain of iodine by weighing the capture substrate before and after iodine loading was deemed to be unreliable due to the tendency for the substrate to absorb water vapour, in particular as the excess iodine was volatilised.

### 2.2. HIP canisters

Nickel and copper were chosen as HIP canister materials, being less likely metals than iron to reduce the wasteform at the edge of the can, available at reasonable cost, and with melting points compatible with the sodalite formation temperature range around 750–950 °C. HIP canisters were machined from 99.0% purity nickel rod and 99.9% purity copper tube and rod – the tube being used for the can walls and the rod for the end caps. The internal diameter and height of the HIP canisters were 16 mm and 50 mm respectively. HIP canisters of these dimensions were used to ensure that a complete radial slice could be cut from the HIP can, thus preserving the wasteform/HIP canister interface. In addition, a 45 mm internal diameter by 50 mm height copper HIP canister was machined from copper rod. This provided a core sample of the HIPed wasteform that was free from any wasteform/HIP canister interactions for use in standard aqueous durability (PCT and MCC) tests.

The iodine loaded zeolite was uniaxially pressed into the HIP canisters. End caps with evacuation tubes were welded onto the HIP canisters, and all HIP canisters were baked out under vacuum for 4 h at 500 °C to remove moisture. Open furnace trials indicated that loss of silver iodide at this temperature was minimal.

The HIP cycle heated at 5 °C per minute to 900 °C (nickel cans) or 750 °C (copper cans), a 2 h dwell with 100 MPa applied pressure, and cooling at 5 °C per minute until thermal transfer limits meant that natural cooling rates were slower than this. The lower temperature for the copper cans was chosen to avoid any risk of HIP canister breaches due to the silver − copper eutectic that forms at 780 °C.

### 2.3. Sample characterisation

From a sample fabrication perspective, the main area of microstructural interest was to establish whether any interfacial reactions would occur between the silver sodalite and the metal HIP canister walls. The principal microstructural characterisation tools used for this were scanning electron microscopy (SEM) coupled with energy dispersive spectroscopy (EDS). X-ray diffraction (XRD) and SEM were both used to characterize the bulk material and confirm that silver sodalite had formed as the predominant phase.

SEM was carried out on cross-sectioned samples cut from the small HIP canisters, mounted in epoxy resin, polished to a 1 μm-diamond finish and coated with approximately 5 nm of carbon to avoid charging effects. The SEM was a Zeiss Ultra Plus instrument operating in back scattered electron mode, with an attached Oxford Instruments X-Max 80 $mm^2$ SDD X-ray microanalysis system operated at an accelerating voltage of 15 kV.

XRD was carried out using a Panalytical X'Pert instrument (Cu Kα radiation) operating at 45 kV and 40 mA.

### 2.4. Leach testing

Leach tests were conducted on material free from any wasteform/HIP canister interactions and this material was retrieved from the core of the large copper canister.

7-day PCT-B leaching experiments [22] were conducted at 90 °C on 75–150 μm granules of the consolidated wasteform which had been washed in cyclohexane to remove fines. Tests were carried out in triplicate using (a) deionised water and (b) deionised water to which 0.5 g of fine Fe (<450 μm), Cu (<150 μm) or Ni powders (−200 + 325 mesh) were added, creating a range of reducing conditions to see if iodine leaching was enhanced relative to deionised water, as is the case for AgI [23]. Ag, Al and Si concentrations in the leachate were analysed using a Perkin Elmer Optima 5300DV ICP-OES calibrated between 0.05 and 100 ppm using wavelength lines 328.068, 396.153 and 251.611 nm, respectively. The flow rates for the plasma, auxilary and nebuliser gases were 15, 0.2 and 0.75 $L.min^{-1}$, respectively. The generator power was 1400 W, and the peristaltic pump sample flow rate was 1.8 mL $min^{-1}$. Samples were run in triplicate in a $HNO_3$ matrix at 100x dilution.

MCC-1 leach tests [24] were conducted on coupons 8 mm square by 2 mm thick with the large faces polished to a 0.25 μm finish, in 20 mL of deionised water at 90 °C.

Iodine concentrations in the leachates were analysed using Neutron Activation Analysis (NAA). 500 μL aliquots were pipetted onto thick filter papers in polyethylene vials and dried. The samples were then irradiated in the OPAL reactor at ANSTO at a thermal neutron flux of $2.2 \times 10^{13}$ $cm^{-2}s^{-1}$ for 30 s. Gamma-ray spectrum measurements were taken after a short decay period. Concentrations of iodine and other elements of interest were quantified using the k0 method of standardisation which enables analysis using only a single comparator element. Dilute Au in Al wires (IRMM-530R) were used as the comparator. Gamma-ray measurements were carried out using ORTEC P-type high purity germanium detectors coupled to ORTEC DSPec Pro digital spectrometers.

### 2.5. Post leaching characterisation

Apart from solution analysis, the powder residues from PCT were analysed by XRD. Post leaching MCC-1 test samples were examined in various ways. Firstly grazing incidence (GI) XRD was conducted on the leached surfaces at 0.5, 1.0 and 2.0° angles of incidence. This corresponds to an X-ray penetration of up to ~1 μm as determined from linear attenuation coefficients and assuming silver sodalite, although the actual interrogation distance would depend on the species formed at the surface following leaching. The same surface was then imaged using standard SEM methods after carbon coating of a few nm. Finally, cross sectional SEM was conducted on the leached surfaces: sections for cross-sectional SEM were prepared by cutting the sample in half, sandwiching the leached layers together (in an attempt to protect the layer) and then polishing. Given the friability of the leached layer, this inevitably led in some cases to removal of a large portion of the leached layer.

The reduction potential (Eh) of experimental solutions after durability/product consistency testing was measured at 20 °C using a Metrohm combined platinum ring electrode (with reference system Ag/AgCl/c(KCl) = 3 M) and converted to Standard Hydrogen Electrode (SHE) values.

## 3. Results and discussion

This study has focussed on a candidate wasteform for iodine immobilisation produced from a commercial iodine vapour capture substrate. Previous work [18] has demonstrated that iodine loaded commercial silver exchanged zeolite could be converted to silver sodalite after HIPing in Fe HIP canisters at 900 °C and at 100 MPa pressure. Iodine was inhomogeneously distributed however, meaning that iodine rich regions converted to the intended sodalite phase but also contained small inclusions of silver iodide and silica. Iodine free regions, representing the iodine free zeolite beads, were predominantly nepheline ($(Ag,Na)AlSiO_4$) and $SiO_2$. Also noted in this study [18] was the significant interaction zone following the chemical reaction of the wasteform material and the Fe HIP canister. The interaction zone extended ~100 μm from the HIP canister internal wall and into the wasteform material and contained layers of various phases including iron oxide, silver metal and silica. The formation of Ag metal is due to the reducing conditions prevailing in the Fe can at the interface which destabilises silver sodalite with corresponding oxidation of Fe to iron oxide. In the present work Cu and Ni were selected as the HIP canister materials in an attempt to reduce the potential for silver sodalite destabilisation.

### 3.1. Sample preparation

The main observation during sample preparation is that there was no free iodine observed after the initial vapour impregnation stage, and that the iodine loaded zeolite was somewhat darker in colour than had been observed during the initial studies reported in Ref. [18]. The dark colour was lost during the post impregnation heat treatment, which suggested the excess iodine had initially condensed on the zeolite during cooling and then volatilised during the second heat treatment. All of the HIP canisters consolidated successfully with negligible porosity observed in the final form.

### 3.2. Microstructural characterisation

#### 3.2.1. Bulk material

XRD analyses of the core material from both the Cu and Ni canisters were similar and confirmed that the major phase formed was silver sodalite ($Ag_4Al_3IO_{12}Si_3$, JCPDS 00-033-1164), with minor silver iodide inclusions (JCPDS 00-009-0374), Fig. 1. The major difference between the two samples was the slightly enhanced AgI in the material from the Cu canister while the material from the Ni canister showed some evidence in the pattern for nepheline (JCPDS 00-035-0424). Minor amounts of Ag metal could not be definitively observed due to peak overlap with silver sodalite.

SEM analysis of the core material from the Cu HIP canister is shown in Fig. 2, and is consistent with the XRD analysis and previous work. The iodine loaded zeolite consolidated to a mixture of primarily silver sodalite with silver iodide inclusions. The microstructure also contains regions of free silica, consistent with the theoretical mass balance exercise [18]. Small inclusions of silver metal were also observed suggesting that even with a copper HIP canister the reducing effect of the HIP canister walls extends further than the more substantial effects nearer to the HIP canister walls, as discussed in the following sections. The presence of some iodine free regions (zone B in Fig. 2(a)) in the core material was somewhat surprising given attempts were made to saturate the substrate with iodine. As expected from the zeolite stoichiometry, these iodine-free regions converted to silver nepheline and silica during HIP consolidation. Similar results (not shown) were found for the core material taken from the Ni HIP canister. It is important to note here that it was always the intention to produce a realistic candidate wasteform in this study rather than a homogeneous, phase pure product. As such, this inhomogeneity reflects what would be expected to occur in a practical application.

#### 3.2.2. Wasteform/HIP canister interfaces

SEM images of the wasteform/HIP canister interfaces are shown in Figs. 3 and 4. The primary observation is that both nickel and copper destabilise the silver sodalite phase within ~100–200 μm from the internal canister wall, but the resulting microstructures are clearly different for the different canister materials. The Cu canister exhibits a 20–50 μm thick $Cu_2O$ layer immediately adjacent to the HIP canister. The presence of $Cu_2O$ was observed as far as ~150 μm into the wasteform material, demonstrating its high mobility during HIP consolidation. A significantly enhanced amount of Ag metal was noted in the first 200 μm region from the Cu HIP canister, presumably due to the reducing conditions caused by the Cu canister at the interface which destabilises Ag sodalite. This is in line with the oxidation of the Cu HIP canister material. The presence of Ag metal is significantly reduced outside of the wasteform/HIP canister interaction zone, although Ag metal was also noted as rings around the AgI sodalite zones suggesting that the effects of the HIP canister material extend well into the bulk of the wasteform.

In comparison to that for the Cu canister, the size of the wasteform/HIP canister interaction zone appeared to be somewhat reduced for the Ni canister. A partial Ag metal layer of <5 μm thick was observed, in sections, immediately adjacent to the HIP canister internal wall. Both NiO and Ag metal were consistently observed for the next 50–100 μm from the HIP canister internal wall with larger lumps of Ag metal at distances of ~100 μm from the canister wall.

Detailed mechanisms by which the HIP canister locally destabilises the silver sodalite have not been established in this study. It is, however, interesting to note that the extent of the alteration effects appear to be dependent on more than just the canister materials' relative positions on the electrochemical scale; and this is made more surprising by the fact that the nickel canister was HIPed at 150 °C higher. The extent of wasteform/HIP canister interaction is thus the result of a combination of several factors that include:

1. Reduction potential for the HIP canister material
2. The formation of a "protective" oxide layer on the canister internal wall, for example the 20–50 μm $Cu_2O$ layer
3. HIP consolidation processing conditions and this is not limited to absolute temperature. Rather, it may be relevant that the HIP temperatures were much closer to the melting points of Cu than of Ni so that the atomic mobilities in the metals would be higher for Cu than for Ni.

A more extensive study of temperature, time at temperature and pre-oxidation of the HIP canisters could identify HIP parameters that lead to silver sodalite formation with minimal HIP canister interaction; and such a systematic (T,t) matrix could lead to some understanding of the silver sodalite formation and destabilisation mechanism.

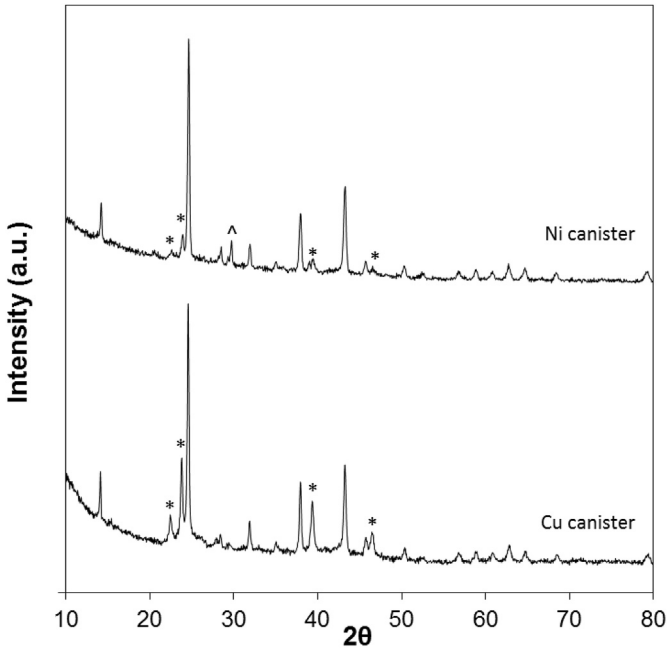


**Fig. 1.** X-ray diffraction pattern of the bulk wasteform material following HIPing in Cu and Ni HIP canisters. All unlabelled peaks are due to Ag sodalite, peaks for AgI (*) and nepheline (^) are also labelled.

### 3.3. Durability assessment of the HIPed product

#### 3.3.1. PCT-B leaching results

PCT leaching experiments [22] at 90 °C were carried out in aqueous media by prescribed protocols. In addition to the standard water experiment, 0.5 g of either Cu, Ni or Fe powder were added to the PCT leaching experiment to investigate the effect of reducing conditions on the leaching value. The results from Eh measurements of the leachate solutions are summarised in Table 1. The PCT leach values for Al, Si, Ag and I are also provided in Table 1 and are all generally very low, as expected for Ag sodalite. However, as found previously for AgI [23], silver sodalite [17] and CuI [15], the highly reducing conditions of the experiment containing Fe powder produced high iodine release to the leachate. The other notable aspect is the slightly enhanced Si release for the Cu buffered experiment when compared to iodine release under other conditions.

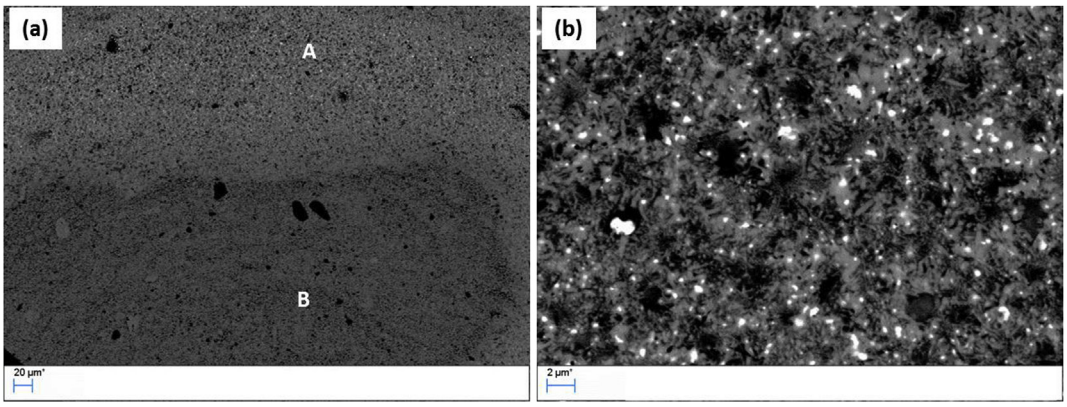


**Fig. 2.** Backscattered SEM at different magnifications from the body of the Cu canister. In (a) zone (A) is a fine grained mixture of AgI, Ag metal, $SiO_2$ and AgI sodalite, while zone (B) is Ag nepheline and $SiO_2$ (black). Zone (A) is enlarged in (b) to show $SiO_2$ (dark), AgI sodalite (mid-grey) and bright specks of Ag metal and AgI.

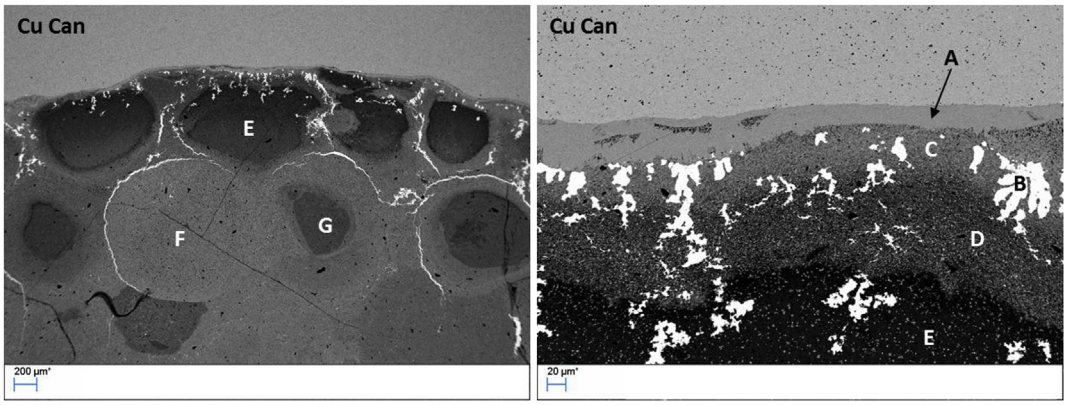


**Fig. 3.** Backscattered SEM images at different magnifications showing the $Cu_2O$ layer (A) at the Cu canister border. In addition, the bright areas (B) are Ag metal. Zones (C) and (D) contain $SiO_2$ (dark), $Cu_2O$ (mid-grey), and aluminosilicate, with significantly more $Cu_2O$ in zone (C). Zone (E) contains $SiO_2$ and Ag nepheline (dark) and mid-grey crystals of $Cu_2O$. In the body of the canister, zone (F) is a fine grained mixture of AgI, Ag metal, AgI sodalite which is ringed by Ag metal and AgI, while zone (G) is Ag nepheline and $SiO_2$.

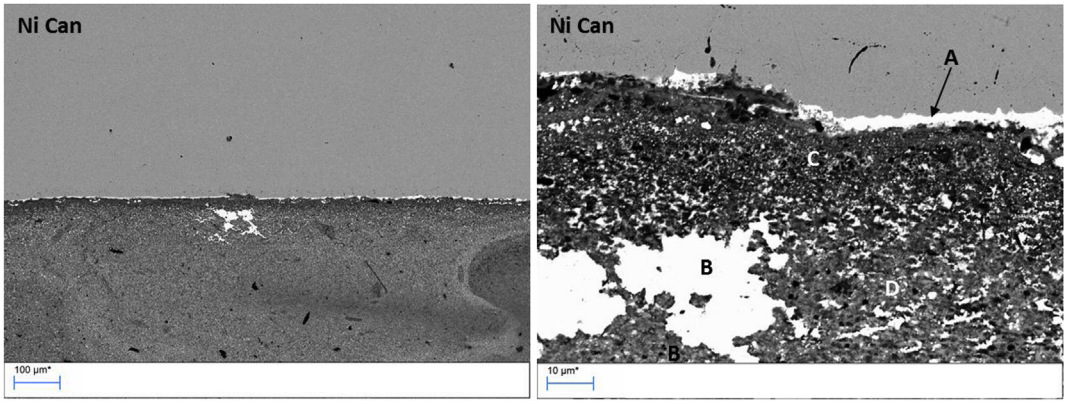


**Fig. 4.** Backscattered SEM images at different magnifications showing the Ag metal layer at the Ni can border. The bright area (A) is a Ag metal layer, with large lumps of Ag metal (B) also present. The darker area (C) is aluminosilicate rich (Al:Si 1:2) with a small amount of NiO and bright specks of Ag metal. The main area (D) is made up of AgI sodalite (mid-grey), $SiO_2$ (dark), and bright AgI and Ag metal.

In an attempt to better understand the reaction occurring under reducing conditions, XRD analysis of the dried and leached material was undertaken in order to identify the solid reaction products. The patterns for the various samples are displayed in Fig. 5.

XRD analysis of the wasteform residues, Fig. 5, revealed that both unbuffered and Ni buffered tests had no significant effect on the wasteform, shown by the fact that the residue was predominantly Ag-sodalite (JCPDS 00-033-1164) rich in both cases. By contrast, Fe and Cu buffered leach tests have destabilised the sodalite phase and left a residue containing mostly Ag metal (JCPDS 03-065-2871) and AgI (JCPDS 00-009-0374) for the Cu buffered experiment and primarily Ag metal for the Fe buffered experiment. The destabilisation of silver sodalite appears most significant in the Fe buffered experiment in agreement with the PCT leach

**Table 1**
PCT leach results for HIPed Ag sodalite with 0.5 g metal powders added to 10 mL deionised water.

| Element | Upper limit on normalised concentration (g/L) | | | |
|---|---|---|---|---|
| | Metal Free | Cu addition | Ni addition | Fe addition |
| Al | 0.00015 | 0.008 | 0.00007 | 0.0015 |
| Si | 0.146 | 0.800 | 0.310 | 0.160 |
| Ag | 0.000121 | 0.0000013 | 0.000095 | 0.000015 |
| I | 0.007 | 0.007 | 0.006 | 100 |
| Eh (mV) | – | 228.6 | 377.6 | −110 |

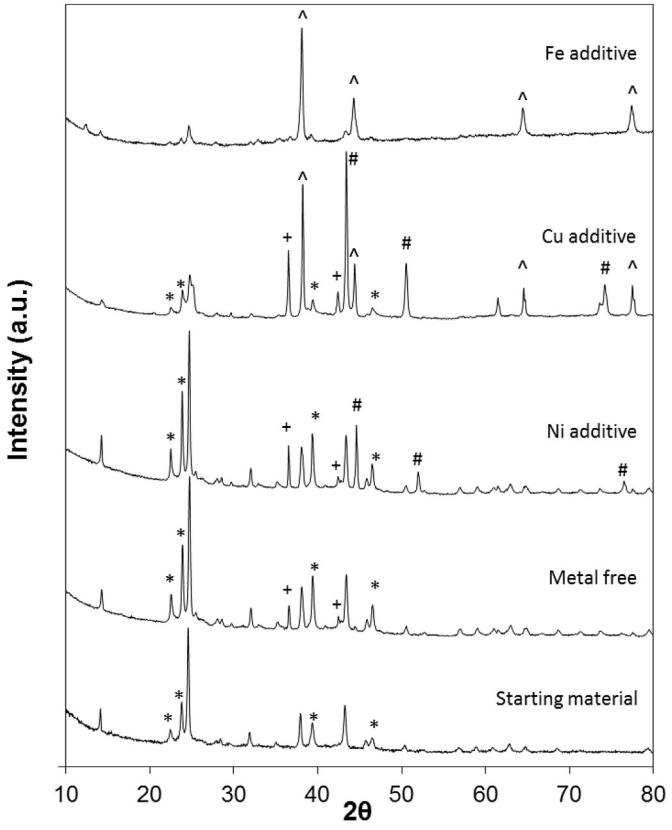


**Fig. 5.** X-ray diffraction pattern of the dried leached powder following the PCT experiment. All unlabelled peaks are due to Ag sodalite, peaks for AgI (*), Ag metal (^), corresponding metal additive (#) are also labelled. An unknown is marked with (+).

experiment results and the quantitative release of iodine to the leachate. Peaks in the corresponding XRD patterns were also noted for the Ni and Cu metal additives.

It was not possible to identify any phase in the XRD patterns that result from the aluminosilicate framework (see for example the pattern from the Fe buffered experiment in Fig. 5) which suggests it has been converted into an amorphous gel. It is clear that in the Cu buffered sample destabilisation of sodalite has not led to high iodine concentrations in the PCT leach solutions, and this is most likely due to the insolubility of AgI. This is also in agreement with slightly enhanced Si releases. Under what are expected to be the most reducing conditions, the Fe buffer, AgI is now also partially destabilised, hence the resulting high iodine levels in the PCT leachates. We note also that most proposed geological disposal facility concepts will tend to reducing conditions, hence AgI formed by sodalite destabilisation will then decompose, and saline groundwater will also lead to iodine release via halide exchange reactions.

**Table 2**
MCC leach results for HIPed Ag sodalite with 0.5 g metal powders added to 10 mL deionised water.

| Element | Normalised Release Rate ($g/m^2/d$) | | | |
|---|---|---|---|---|
| | 0–1 day | 1–7 days | 7–28 days | 28–90 days |
| Metal free | | | | |
| Al | 0.079 | 0.044 | 0.022 | 0.005 |
| Si | 0.195 | 0.117 | 0.126 | 0.083 |
| Ag | 0.138 | 0.054 | 0.042 | 0.017 |
| I | <0.03 | <0.005 | <0.0014 | <0.0004 |
| Cu addition | | | | |
| Al | 0.169 | 0.01398 | 0.002857 | 0.00305 |
| Si | 0.51 | 0.212 | 0.0818 | 0.0369 |
| Ag | 0.00013 | 0.000139 | 0.000112 | 0.0000515 |
| I | <0.03 | 0.046 | 0.016 | <0.0004 |
| Ni addition | | | | |
| Al | <0.001 | <0.00017 | <0.00005 | <0.000016 |
| Si | 0.316 | 0.185 | 0.135 | 0.0181 |
| Ag | <0.00027 | <0.00238 | <0.001117 | 0.000584 |
| I | <0.03 | <0.005 | <0.002 | <0.0004 |
| Fe addition | | | | |
| Al | <0.001 | 0.00214 | <0.00005 | Fragmented |
| Si | 1.02 | 0.275 | 0.0206 | Fragmented |
| Ag | <0.0001 | 0.000034 | 0.000008 | Fragmented |
| I | 261 | 131 | 7.2 | Fragmented |

### 3.3.2. MCC-1 leaching results

Leaching experiments were also conducted according to the MCC-1 test protocol with monolithic samples. This experiment has a low surface area: water volume ratio and is used in conjunction with the PCT experiments. The leached monoliths also provide the opportunity to gain insight into the dissolution mechanisms involved in the leaching process, via characterisation of the leached surfaces of the 90 day MCC-1 samples. The MCC-1 data are shown in Table 2.

As with the PCT-B tests, the key values are the iodine release rates and these are high only for the Fe buffered leach test, when both the sodalite and AgI are destabilised. Moreover, by the 90 day MCC experiment, the Fe buffered sample had completely fragmented. The iodine and initial silicon values from these tests also agree with PCT results in that a Cu buffer leads to higher silicon values, indicating sodalite breakdown, but does not destabilise the resultant AgI.

It is interesting to compare these leach rates with those inferred by Maddrell et al. from predominantly single phase iodide sodalite [11]. To do this we have chosen to compare absolute releases of Si[1] in g $m^{-2}$ of wasteform, to exclude the different normalisation factors applicable to Ag and Na based sodalite. We have used this approach for the first 7 days of leaching because this period matches the available data. For the samples reported here we can look at the unbuffered and Ni-buffered tests because PCT residues indicated these did not significantly destabilise the sodalite. The absolute 7-day elemental loss values are in the range 0.08–0.14 g $m^{-2}$. The figures from Maddrell et al. [11] give a value of 0.16 g $m^{-2}$, which clearly is in good agreement. The leach rates from Maddrell et al. may be slightly higher due to the use of a mildly alkaline leachant, designed to keep leached Al in solution. The overall conclusion is that in the absence of reducing conditions, the silver sodalite produced in this work exhibits comparable durability to what might be regarded as a reference grade sodalite wasteform.

[1] Si has been chosen because, of the wasteform components in silver sodalite, it is the most likely to remain in solution, whereas Ag, I and Al released from the wasteform all appear to precipitate.

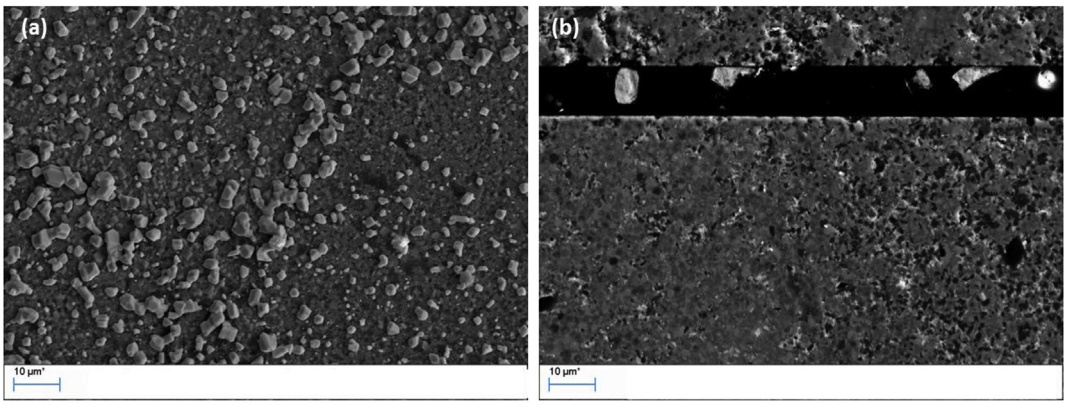


**Fig. 6.** Secondary SEM images of (a) the surface and (b) through the cross-section of the surface of the leached material with no metal buffer added to the leach experiment. In (b) the black strip is the resin between two sandwiched leached surfaces. The main mid-grey phase is silver sodalite, the darker areas are $SiO_2$ rich, and the large particles sitting on the surface in (a) and in the resin between the sandwiched surfaces in (b) are AgI.

### 3.4. Post leaching characterisation

At the end of the 90 day leaching period, the MCC-1 coupons that remained intact (that is, not from the Fe buffered test, see below) were examined by GI-XRD using incident angles of 0.5, 1.0 and 2.0°2θ. This would be expected to interrogate a surface layer of ~1 μm thick and depending on the nature and composition of the surface material. Diffraction signals were often weak due to the poorly crystalline state of many of the alteration products, however the general observations are summarised here. For the leaching experiment with no metal additive (metal free), various apparently AgI phases were noted as well as trace gamma-$Al_2O_3$. No Ag metal was observed in the GI XRD pattern for this sample in agreement with the XRD results obtained from PCT residues. The Cu buffered sample showed peaks corresponding to AgI, Ag metal and Cu metal also in agreement with leached PCT powder residue. Again, possible trace gamma-$Al_2O_3$ was observed. The Ni buffered sample similarly showed peaks in the GI XRD pattern for AgI and Ni metal as well as evidence for $Ni_5Al_4O_{11}.18H_2O$. No GI XRD experiments were undertaken on the Fe buffered leached sample as it had completely lost integrity by the 90 day mark. These GI XRD results are generally similar to those obtained for the powder residues from PCT leach experiments aside from the observation of trace gamma-$Al_2O_3$ in the metal-free and Cu buffered experiments and $Ni_5Al_4O_{11}.18H_2O$ in the Ni buffered experiment.

The leached surfaces of the 90 day MCC-1 samples were then examined using SEM. SEM images were taken from both the surface as well as through the cross-section of the surface in an attempt to obtain information on possible alteration products, see Figs. 6–8).

There was little evidence for any alteration layer on the surface of the 90 day MCC sample experiment without metal buffer (see Fig. 6). Particles of ~5 μm in size were scattered across the surface of the sample and EDS analysis suggested these were AgI, in agreement with GI XRD results. Similar particles were noted in the SEM image of the cross-sectioned sample in the resin area between the sandwiched surfaces. Although the starting material contained some AgI, as determined from XRD analysis, these particles appear to be precipitates of AgI redeposited as alteration products on the surface of the leached material.

Similarly for the Ni buffered 90 day MCC sample, particles of ~50–100 μm in size were observed scattered across the surface of the sample, Fig. 7, and again EDS analysis suggested these were AgI. Similarly, these particles appear to be AgI redeposited on the surface of the leached material. This also agrees with the GI XRD results described above. In addition, a fine aluminosilicate deposit was noted on the surface of the sample and this appeared as a ~5–10 μm thick alteration layer in the cross-section image of Fig. 7(b). The measured composition of this layer had atomic ratios of ~2:3:4 Al:Si:Ni.

The surface of the Cu buffered 90 day MCC leached sample was similarly covered in AgI particles up to ~10 μm in size (see Fig, 8). There was no clear alteration layer observed via SEM analysis of the surface of the sample, however an alteration layer of 2–5 μm thick was noted (in areas) in the cross-sectioned sample. The composition of this aluminosilicate alteration layer was measured to have an atomic ratio of ~2:3:10 Al:Si:Cu.

## 4. Further discussion and conclusions

Consolidation of iodine loaded silver exchanged zeolite into a sodalite wasteform by hot isostatic pressing was achieved with a waste loading of ~15 wt%. Although it was confirmed that conversion to a primarily silver sodalite wasteform occurs there are caveats as to the attractiveness of the process. The production of the sodalite wasteform was accompanied by the formation of an interfacial reaction zone of up to ~200 μm in thickness between the HIP canister and wasteform. This interaction was observed even with metal canisters such as Cu and Ni and was characterised by some destabilisation of the sodalite at the interface with the HIP canister. Potentially this destabilisation could be minimised by using lower HIP temperatures, if such processing does not lead to poor consolidation and this will be investigated in future work.

A further concern is the long term durability as leaching results indicate that reducing conditions readily destabilise the silver sodalite, and most proposed geological disposal environments will indeed be reducing - although it should be emphasised that silver sodalite is not inferior to the popular AgI-based candidate wasteforms in this respect. Initially the sodalite framework was observed to be destabilised under the reducing leaching conditions produced by Ni and Cu metal buffers, with concomitant formation of AgI and an aluminosilicate alteration layer. AgI was observed as particles redeposited on the surface of the leached monolithic samples and did not lead to high iodine concentrations in the leach solutions. This is likely due to the insolubility of AgI. Under the more highly reducing conditions obtained with an Fe metal buffer, AgI was also partially destabilised and resulted in high iodine release to the leachates.

It is worth mentioning that whilst Cu and Ni HIP canisters will both be expected to have significant lifetimes under such repository conditions, our overarching philosophy when assessing

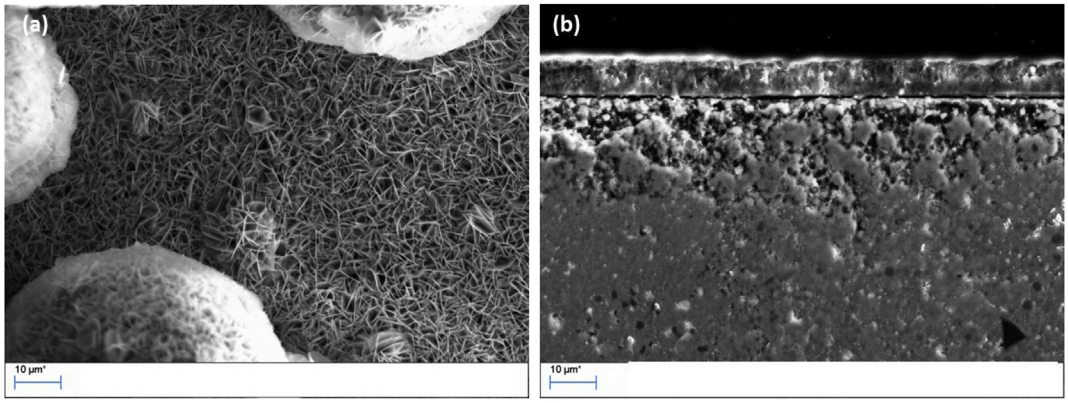


**Fig. 7.** Secondary SEM images of (a) the surface and (b) through the cross-section of the surface of the leached material with Ni metal buffer added to the leach experiment. The large particles of AgI and fine micron needles are aluminosilicate material.

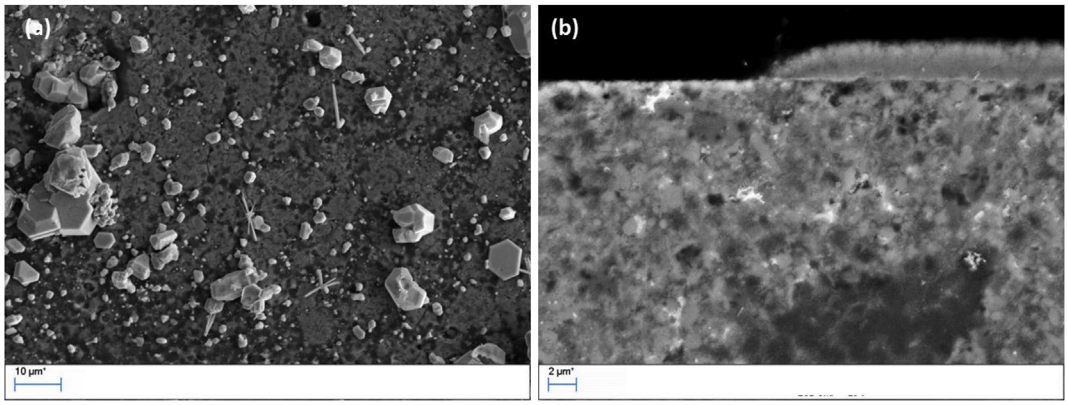


**Fig. 8.** Secondary SEM images of (a) the surface and (b) through the cross-section of the surface of the leached material with Cu metal buffer added to the leach experiment. In (b) a partial aluminosilicate alteration layer is observed. The main mid-grey phase is silver sodalite, the darker areas are $SiO_2$ rich, and the large particles sitting on the surface in (a) are AgI.

the performance of a candidate wasteform is not to consider any benefit that the HIP canister could potentially provide to the material within it. Utilisation of this candidate silver sodalite wasteform under these reducing repository conditions would therefore require some modification of the wasteform's local environment, for example by adding a redox buffer (such as $Fe_2O_3$ powder) to the area surrounding the HIP canisters [25].

An alternative may be to dilute the AgI sodalite in porous titania or alumina beads which can then be consolidated to give silver iodide particles encapsulated in a durable matrix. This approach may require the use of aqueous/hydrothermal routes to form the sodalite phase, for example those investigated by Nam et al. [26]. The routes would need to be optimised to maximise the incorporation of iodine “per cycle” plus designed to eliminate/minimise effluent discharges. The solid formed by these synthesis methods would then need to be retrieved, dried and consolidated to produce the final wasteform, for which HIP would be the most suitable method.

## Acknowledgments

The authors wish to acknowledge K. Lu for preparing SEM samples.

## References

[1] B.J. Riley, J.D. Vienna, D.M. Strachan, J.S. McCloy, J.L. Jerden, J. Nucl. Mater. 470 (2016) 307.
[2] H. Tanabe, T. Sakuragi, K. Yamaguchi, T. Sato, H. Owada, Adv. Sci. Technol. 73 (2010) 158.
[3] R.T. Jubin, Airborne Waste Management Technology Applicable for Use in Reprocessing Plants for Control of Iodine and Other Off-Gas Constituents, 1988. ORNL/TM-10477.
[4] Patricia Paviet-Hartmann, William Kerlin, Steven Bakhtiar, Treatment of Gaseous Effluents Issued from Recycling – A Review of the Current Practices and Prospective, 11th Actinide and Fission Product Partitioning and Transmutation Exchange Meeting Improvements, Nov 2010. INL/CON-10-19961.
[5] D.R. Haefner, T.J. Tranter, Methods of Gas Phase Capture of Iodine from Fuel Reprocessing Off-Gas: A Literature Survey, Idaho National Laboratory, 2007.
[6] K.W. Chapman, P. Chupas, T. Nenoff, Radioactive Iodine Capture in Silver containing mordenites through nanoscale silver iodide formation, J. Am. Chem. Soc. 132 (2010) 8897–8899.
[7] P. Taylor, A Review of Methods for Immobilizing Iodine-129 Arising from a Nuclear Fuel Recycle Plant, with Emphasis on Waste-form Chemistry, AECL-10163, 1990 ([AECL Internal Report]).
[8] T. Nakazawa, H. Kato, K. Okada, S. Ueta, M. Mihara, in: In Scientific Basis for Nuclear Waste Management XXIV, Materials Research Society Proceedings, vol. 663, 2001, pp. 51–57.
[9] H. Babad, D.M. Strachan, U.S. Patent 4 (229) (1980) 317.
[10] V.A. Suvorova, V.N. Zyryanov, A.R. Kotelnikov, Engineering geology and the environment, in: Koukis Marinos (Ed.), Tsiambaos & Stournaras, Publ. Balkema, Rotterdam, 1997, pp. 2199–2202.
[11] E.R. Maddrell, A.S. Gandy, M.C. Stennett, J. Nucl. Mater. 449 (2014) 168–172.
[12] B.J. Riley, J. Kroll, J. Peterson, J. Matyáš, M. Olszta, X. Li, J.V. Vienna, Silver-loaded aluminosilicate aerogels as iodine sorbents, ACS Appl. Mater. Interfaces 9 (38) (2017) 32907–32919.
[13] J. Matyáš, N. Canfield, S. Sulaiman, M. Zumhoff, Silica-based waste form for immobilisation of iodine from reprocessing plant off-gas streams, J. Nucl. Mater. 476 (2016) 255–261.
[14] H. Yang, H.-S. Park, Y.-Z. Cho, Silver phosphate glasses for immobilisation of radioactive iodine, Ann. Nucl. Energy 110 (2017) 208–214.

[15] E.R. Vance, C. Grant, I. Karatchevtseva, Z. Aly, A. Stopic, J. Harrison, G. Thorogood, H. Wong, D.J. Gregg, Immobilisation of iodine via copper iodide, J. Nucl. Mater. 505 (2018) 143–148.
[16] E.R. Maddrell, Fabrication of potential iodine wasteforms by hot isostatic pressing, BNFL Internal Report RAT 3104 (2002).
[17] E.R. Vance, D.J. Gregg, C. Grant, A. Stopic, E.R. Maddrell, Silver iodide sodalite for 129I immobilisation, J. Nucl. Mater. 480 (2016) 177.
[18] E.R. Maddrell, E.R. Vance, D.J. Gregg, J. Nucl. Mater. 467 (2015) 271–279.
[19] E. Kuo, D. Gregg, E. Vance, E. Maddrell, G. Lumpkin, Radioactive iodine-129 capture in mixed cation sodalites: ab initio modelling, MRS Advances 3 (20) (2018) 1105–1110, https://doi.org/10.1557/adv.2018.249.
[20] Y. Zhang, H. Li, S. Moricca, J. Nucl. Mater. 377 (2008) 470–475.
[21] Y. Zhang, M.W.A. Stewart, H. Li, M.L. Carter, E.R. Vance, S. Moricca, J. Nucl. Mater. 395 (2009) 69–74.
[22] ASTM C 1285 – 14. "Standard Test Methods for Determining Chemical Durability of Nuclear, Hazardous, and Mixed Waste Glasses and Multiphase Glass Ceramics: the Product Consistency Test (PCT)". ASTM International..
[23] H. Tanabe, T. Sakuragi, K. Yamaguchi, T. Sato, H. Owada, Adv. Sci. Technol. 73 (2010) 158.
[24] ASTM C1220-10, Standard Test Method for Static Leaching of Monolithic Wasteforms for Disposal of Radioactive Waste, ASTM International, 2010.
[25] Saewha et al ref.
[26] S. Chong Nam, B.J. Riley, J.S. McCloy, MRS Advances 3 (Issue 20) (2018) 1093–1103.